

Direct Observation of Substrate–Enzyme Complexation by Surface Forces Measurement¹

Takehiro Suzuki,^{†,‡} Yuan-Wei Zhang,[†] Tanetoshi Koyama,[†] Darryl Y. Sasaki,[§] and Kazue Kurihara^{*,†}

Contribution from the Institute for Multidisciplinary Research for Advanced Materials, Tohoku University, 2-1-1 Katahira, Aoba-ku, Sendai 980-8577, Japan, and Biomolecular Materials Department, Sandia National Laboratories, MS 1413, Albuquerque, New Mexico 87185

Received March 16, 2006; E-mail: kurihara@tagen.tohoku.ac.jp

Abstract: The substrate–enzyme complexation of heptaprenyl diphosphate synthase was directly investigated using colloidal probe atomic force microscopy (AFM) and a quartz crystal microbalance (QCM) in order to obtain new insights into the molecular mechanism of the enzyme reaction. This enzyme is composed of two dissociable subunits that exhibit a catalytic activity only when they are associated together in the presence of a cofactor, Mg²⁺, and a substrate, farnesyl diphosphate (FPP). The QCM measurement revealed that FPP was preferentially bound to subunit II in the presence of Mg²⁺, while the AFM measurement showed that the adhesive force between the subunits was observed only in the presence of both Mg²⁺ and FPP. This is the first direct demonstration of the specific interaction involved in the enzyme reaction. The dependence of the Mg²⁺ concentration on the specific interaction between subunits I and II well agreed with that on the enzyme activity of heptaprenyl diphosphate synthase. This indicated that the observed adhesive forces were indeed involved in the catalytic reaction of this enzyme. On the basis of these results, we discussed the processes involved in the substrate–enzyme complexation. The first, the substrate FPP bound to subunit II using Mg²⁺, followed by the formation of the subunit I–FPP–Mg²⁺–subunit II complex. Our study showed a very useful methodology for examining the elemental processes of biological reactions such as an enzyme reaction.

Introduction

The elucidation of specific interactions involved in biological reactions is essential in biological science. Especially, the interactions between protein molecules have attracted increasing attention as the importance of proteome research is now becoming widely acknowledged. The essential questions include, (1) what protein pairs interact, (2) how do they recognize each other, (3) what are the locations and the sequence of a binding site, and (4) what are their functions?

The interactions of proteins and other biomolecules have been actively studied using both the conventional and novel nanoscale measurements. They include ultracentrifugation,² surface plasmon resonance (SPR),³ and a quartz-crystal microbalance (QCM).⁴ Among them, the atomic force microscopy (AFM)⁵ and surface forces measurement (SFA)⁶ occupy a unique

position, because they can directly monitor interaction forces by employing a spring balance. However, the protein systems studied so far are rather limited to relatively simple ones such as the interactions between antigen–antibody^{7,8} or protein unfolding.^{9–11} It is important to further develop the potential of this measurement for studying biological systems. This is the primary aim of the current study. We employed the force measurement for studying the interactions and elementary processes involved in the enzymatic reaction.

Prenyltransferases (prenyl diphosphate synthases) catalyze the sequential head-to-tail condensation of isopentenyl diphosphate (IPP) with allylic substrates to give linear prenyl diphosphates in the biosynthetic pathway of isoprenoid compounds. Although these condensation reactions are similar in terms of their chemical mechanism, there are a number of enzymes having different specificities of substrates and products with respect to the chain length and double-bond stereochemistry.¹² Among the prenyltransferases, medium-chain (*E*)-prenyl diphosphate synthases are unusual because of their heteromeric structures. Heptaprenyl diphosphate (HepPP) synthase from *Bacillus sub-*

* To whom correspondence should be addressed.

[†] Tohoku University.

[‡] Current address: National Institute for Environmental Studies, 16-2 Onogawa, Tsukuba City, Ibaraki 305-8506 Japan.

[§] Sandia National Laboratories.

- (1) Primary account of this work: Suzuki, T.; Zhang, Y.-W.; Koyama, T.; Sasaki, D. Y.; Kurihara, K. *Chem. Lett.* **2004**, *33*, 536.
- (2) Rivas, G.; Stafford, W.; Minton, A. P. *Methods* **1999**, *19*, 194.
- (3) Smith, E. A.; Thomas, W. D.; Kiessling, L. L.; Corn, R. M. *J. Am. Chem. Soc.* **2003**, *125*, 6140.
- (4) Yun, Z.; Vladislav, T.; Megahna, S.; Xiangqun, Z.; George, W. P. *J. Am. Chem. Soc.* **2003**, *125*, 9292.
- (5) Binnig, G.; Quate, C. F.; Gerber, C. *Phys. Rev. Lett.* **1986**, *56*, 2048.
- (6) Israelachvili, J. N.; Adams, G. J. *Chem. Soc., Faraday Trans. 1* **1978**, *74*, 975.

- (7) Moy, V. T.; Florin, E.-L.; Gaub, H. E. *Science*, **1994**, *266*, 257.
- (8) Wong, J.; Chilkoti, A.; Moy, V. T. *Biomol. Eng.* **1999**, *16*, 45.
- (9) Oberhauser, A. F.; Marszalek, P. E.; Carrion-Vazquez, M.; Fernandez, J. M. *Nat. Struct. Biol.* **1999**, *6*, 1025.
- (10) Rief, M.; Gautel, M.; Gaub, H. E. *Adv. Exp. Med. Biol.* **2000**, *481*, 129.
- (11) Oesterhelt, F.; Oesterhelt, D.; Pfeiffer, M.; Engel, A.; Gaub, H. E.; Müller, D. J. *Science* **2000**, *288*, 143.
- (12) Ogura, K.; Koyama, T. *Chem. Rev.*, **1998**, *98*, 1263.

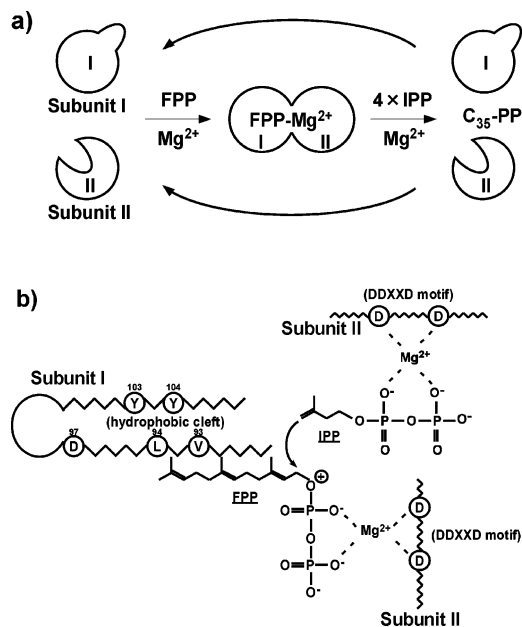


Figure 1. (a) Hypothetical mechanism of the catalytically active complex of HepPP synthase of *B. subtilis*.¹⁶ (b) Hypothetical scheme for the binding of FPP and IPP between the two subunits of *B. subtilis* HepPP synthase.^{23,24} D is aspartic acid.

tilis (*B. subtilis*),^{13–15} which forms the HepPP with a chain length of C₃₅, is composed of two nonidentical protein subunits, neither of which has a catalytic activity alone. These subunits have been assumed to associate in the presence of a substrate, allylic substrate (*E,E*)-farnesyl diphosphate (FPP), and a co-factor, Mg²⁺, to form a catalytically active complex, which represents an intermediate state during the catalysis (Figure 1a).¹⁶ This catalytically active complex has been characterized by the gel filtration and cross-linking experiments.¹⁶ However, there has been no direct evidence to support the assumption that the two subunits would associate to form a transient dimer by specific interactions between them. Concerning this enzyme–substrate, it should be interesting to study the following: (1) how two subunits interact with each other; (2) which subunit participates in the enzyme reaction; and (3) how the substrate (FPP) binds to the subunit (or subunits).

Recently, the crystal structure of avian FPP synthase complexed with allylic substrates has been analyzed,¹⁷ and it has been shown that allylic diphosphates bind through Mg²⁺ to the aspartates of the conserved Asp-rich motif (DDXXD), which are essential and highly conserved among the (*E*)-prenyl diphosphate synthases,^{18–20} with the hydrocarbon tails of the ligands growing in the hydrophobic pocket. Furthermore, the crystal structure of the undecaprenyl diphosphate synthase from *Micrococcus luteus* (*M. luteus*) B-P 26, which is a homodimer and forms a 55-carbon long-chain product, has been shown to give the same result as the FPP synthase.²¹ Though *B. subtilis* HepPP synthase is a heterodimer, subunit II has motifs similar

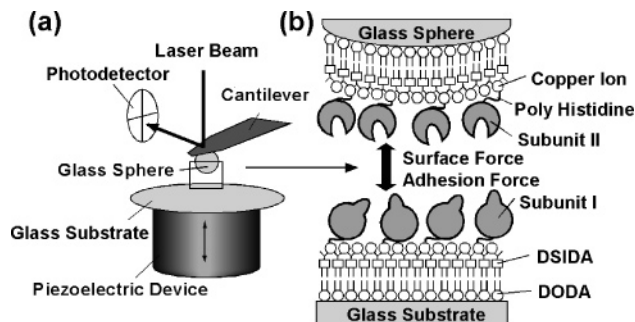


Figure 2. Schematic drawings of experimental setup: surface forces measurement system employing the atomic force microscope (a) and sample surfaces (b). The glass surfaces are driven by the piezoelectric device. Surface force, F , is given as the product of the spring constant of the cantilever, k , and cantilever deflection, ΔD , which is obtained from the direction of the laser light reflected on the back of the cantilever. The laser light is detected by the four-sectored photodiode.

to those of the avian FPP synthase including the two DDXXD sequences.¹⁶ It is reasonable to assume that subunit II has a tertiary structure similar to the subunit of the avian FPP synthase. Therefore, the diphosphate moiety of FPP seems to bind through Mg²⁺ to the DDXXD motif of subunit II. On the other hand, the prenyl tail of FPP seems to be stretched into a hydrophobic pocket or wall containing Val-93, Leu-94, and Tyr-104 in region B of subunit I.^{22,23} Consequentially, the diphosphate moiety of FPP seems to bind through Mg²⁺ to the DDXXD motif of subunit II, and the prenyl tail of FPP binds to a hydrophobic pocket of subunit I (Figure 1b).^{23,24} There is another Mg²⁺ binding site, the DDXXD motif, for IPP in subunit II. When the enzyme–substrate complex is formed, the IPP, which binds to subunit II through Mg²⁺, is condensed to FPP up to four times one after another.²⁴ As a result, HepPP of 35 carbons is synthesized. However, the formation process of the substrate–enzyme complex has not been elucidated.

In this study, we evaluated the molecular mechanism of the enzyme reaction employing a colloidal probe AFM and QCM. We first investigated how FPP binds to subunits I and II in the absence or presence of Mg²⁺ using QCM. The Au electrode of the QCM quartz plates were modified with protein layers as schematically shown in Figure 2. Next, we directly measured the interactions between subunits I and II by a colloidal probe AFM and observed an adhesive force only when both Mg²⁺ and FPP were present in a bathing solution. The effects of Mg²⁺, FPP, and IPP were also investigated.

Experiments

Materials. The two subunits (subunit I and subunit II) of the HepPP synthase of *B. subtilis* were overproduced in *Escherichia coli* (*E. coli*) cells respectively and purified as previously described.¹⁶ These subunits are modified with six histidines (polyhistidine) at the N terminal. (*E,E*)-FPP and IPP were synthesized according to the procedure of Davisson et al.²⁵ The preparation of *N*-(8-(1,2-di(octadecyloxy)propanoxy)-3,6-dioxaoctyl)iminodiacetic acid (DSIDA) was previously described.²⁶

(13) Takahashi, I.; Ogura, K.; Seto, S. *J. Biol. Chem.* **1980**, *255*, 4539.
 (14) Fujii, H.; Koyama, T.; Ogura, K. *FEBS Lett.* **1983**, *161*, 257.
 (15) Zhang, Y.-W.; Koyama, T.; Ogura, K. *J. Bacteriol.* **1997**, *179*, 1417.
 (16) Zhang, Y.-W.; Koyama, T.; Marecak, D. M.; Prestwich, G. D.; Maki, Y.; Ogura, K. *Biochemistry* **1998**, *37*, 13411.
 (17) Tarshis, L. C.; Yan, M.; Poulter, C. D.; Sacchettini, J. C. *Biochemistry* **1994**, *33*, 10871.
 (18) Joly, A.; Edwards, P. A. *J. Biol. Chem.*, **1993**, *268*, 26983.
 (19) Song, L.; Poulter, C. D. *Proc. Natl. Acad. Sci. U.S.A.* **1994**, *91*, 3044.
 (20) Koyama, T.; Tajima, M.; Sano, H.; Doi, T.; Koike-Takeshita, A.; Obata, S.; Nishino, T.; Ogura, K. *Biochemistry* **1996**, *35*, 9533.

(21) Fujihashi, M.; Zhang, Y.-W.; Higuchi, Y.; Li, X.-Y.; Koyama, T.; Maki, K. *Proc. Natl. Acad. Sci. U.S.A.* **2001**, *98*, 4337.
 (22) Koyama, T.; Tajima, M.; Nishino, T.; Ogura, K. *Biochem. Biophys. Res. Commun.* **1995**, *212*, 681.
 (23) Zhang, Y.-W.; Li, X.-Y.; Sugawara, H.; Koyama, T. *Biochemistry* **1999**, *38*, 14638.
 (24) Zhang, Y.-W. Doctoral dissertation, Tohoku University, 1997.
 (25) Davisson, V. J.; Woodside, A. B.; Neal, T. R.; Stremmer, K. E.; Muehlbacher, M.; Poulter, C. D. *J. Org. Chem.* **1986**, *51*, 4768.
 (26) Sheek, D. R.; Pack, D. W.; Sasaki, D. Y.; Arnold, F. H. *Langmuir* **1994**, *10*, 2382.

Diocetadecyldimethylammonium bromide (DODA) was purchased from Sogo Pharmaceutical and used as received. Tris(hydroxymethyl)aminomethane (Tris), NaCl, and MgCl₂ were purchased from Nacalai Tesqu. All other reagents were of analytical grade. The water was purified and distilled twice by a Nanopure II and FI-stream 48D glass still system (Barnstead).

Preparation of Protein-Modified Surfaces. The glass and QCM plate surfaces were modified with DODA and DSIDA-Cu²⁺ monolayers by the Langmuir–Blodgett deposition at 20.0 ± 0.1 °C using a computer-controlled film balance system (NL-BIO20-MWC, Nippon Laser & Electronics). The sample surfaces were prepared by following a previously described procedure.²⁷ The surfaces were rendered hydrophobic by depositing DODA monolayers at a surface pressure of 35 mN/m in the upstroke mode at a rate of 3.0 mm/min. The DSIDA-Cu²⁺ monolayer was transferred to the hydrophobic glass surface at a surface pressure of 40 mN/m from the protein solution subphase (1.0 × 10⁻⁷ M) (M = mol dm⁻¹) in the downstroke mode at a rate of 3.0 mm/min. The concentration of the proteins was chosen to be slightly higher than the concentration, (8 ± 1) × 10⁻⁸ M, for both I and II, which showed the saturated adsorption on the DSIDA-Cu²⁺ monolayer determined by QCM in a 0.1 mM Tris-HCl buffer containing 1.0 mM NaCl (data are not shown). The transfer ratio of the protein-bound DSIDA-Cu²⁺ monolayer on the hydrophobic glass was found to be 0.6 ± 0.1. The surface density of the protein was 2.7 × 10⁻⁸ mol/m².

Adsorption Measurement. The adsorption of FPP by subunits I and II was monitored using a 27-MHz quartz-crystal microbalance (QCM, Initium, AFFINIX Q).²⁸ Both sides of the AT-cut quartz plate (Initium) bore Au electrodes of 2.5 mm diameter (4.9 mm² area). Sauerbrey's eq 1 was used to calculate the mass of the adsorbed molecules.

$$\Delta F = -\frac{2F_0^2}{A\sqrt{\rho_q\mu_q}}\Delta m \quad (1)$$

where ΔF is the measured frequency change (Hz), F_0 is the fundamental frequency of the QCM (27 × 10⁶ Hz), Δm is the mass change (g), A is the electrode area (4.9 mm²), ρ_q is the density of the quartz (2.65 g cm⁻³), and μ_q is the shear modulus of the quartz (2.95 × 10¹¹ dyn cm⁻²). This equation has been obtained for the AT-cut shear mode QCM in the air phase²⁹ and is known to be used for measurements in the aqueous solution.³⁰

Subunits I and II were transferred onto the quartz plate using the LB method, and the frequency changes by adsorption of the FPP were examined in the 0.1 mM Tris buffer solution containing 1.0 mM or 0 mM MgCl₂.

The association constant was determined on the basis of the Langmuir adsorption isotherm using the QCM results, and by fitting them with the equation

$$\frac{C}{y} = \frac{1}{y_m}C + \frac{1}{ky_m} \quad (2)$$

where C , y , y_m , and k are the substrate concentration, binding ratio at concentration C , the maximum binding ratio, and the association constant, respectively.

Surface Forces Measurement. The interaction force (F) between the protein-modified glass sphere and plate was measured as a function of the surface separation distance (D) by the colloidal probe method³¹ using AFM (Seiko II, SPI3700-SPA300). The measurements were

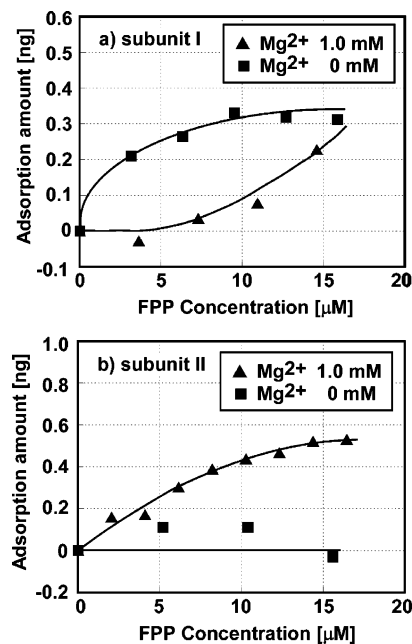


Figure 3. Change in the adsorption amount by the subunit vs FPP concentration in 0.1 mM Tris buffer solution containing 1.0 mM NaCl. ▲, in the presence of 1.0 mM Mg²⁺; ■, in the absence of Mg²⁺ at pH = 8.3: (a) subunit I; (b) subunit II.

carried out basically similar to previous studies.^{27,32} A colloidal glass sphere (Polyscience, 10–20 μm radius) was attached to the top of a cantilever (Olympus, RC-800PS-1) with epoxy resin (Shell, Epikote1004). Interactions between the sphere and a glass substrate (Matsunami, microcover glass) were measured in a homemade closed AFM fluid cell. The obtained forces were normalized by the radius (R) of the sphere using the Derjaguin approximation,³³

$$F/R = 2\pi G_f \quad (3)$$

where G_f is the interaction free energy per unit area between two flat surfaces.

The interactions between the protein-modified surfaces were measured in 0.1 mM Tris-HCl buffer solution (pH = 8.3) containing 1.0 mM NaCl by varying the concentrations of MgCl₂ (cofactor, 0–2.0 mM), FPP (substrate, 0–30 μM), and IPP (another substrate, 0–60 μM; Figure 2).

Results and Discussion

Binding of FPP to Subunits I and II Studied by QCM.

The QCM technique was used to measure the adsorption of FPP by subunits I and II immobilized on the QCM plate in the presence or in the absence of Mg²⁺. Parts a and b of Figure 3 plot the adsorption amount of FPP, calculated from the frequency change, by subunits I and II, respectively. In the absence of Mg²⁺, FPP started to be adsorbed on subunit I at FPP concentrations less than 3.5 μM, and the adsorbed amount reached saturation, i.e., 0.34 ± 0.06 ng, at a 15 μM FPP. On the other hand, in the presence of Mg²⁺, FPP was adsorbed only at concentrations higher than 7 μM. In the case of subunit II, FPP was adsorbed on subunit II only in the presence of Mg²⁺. This result agreed well with the model shown in Figure 1b in which the diphosphate group of FPP binds to the DDXD motif

(27) Ishiguro, R.; Sasaki, D. Y.; Pacheco, C.; Kurihara, K. *Colloids Surf., A* **1999**, *146*, 329.

(28) Okahata, Y.; Niikura, K.; Sugiura, Y.; Sawada, M.; Morii, T. *Biochemistry* **1998**, *37*, 5666.

(29) Sauerbrey, G. Z. *Phys.* **1959**, *155*, 206.

(30) Okahata, Y.; Kawase, M.; Niikura, K.; Ohtake, F.; Furusawa, H.; Ebara, Y. *Anal. Chem.* **1998**, *70*, 1288.

(31) Ducker, W. A.; Senden, T. J. *Langmuir* **1992**, *8*, 1831.

(32) Mizukami, M.; Moteki, M.; Kurihara, K. *J. Am. Chem. Soc.* **2002**, *124*, 12889.

(33) Israelachvili, J. N. *Intermolecular and Surface Forces*, 2nd ed.; Academic Press: London, 1991.

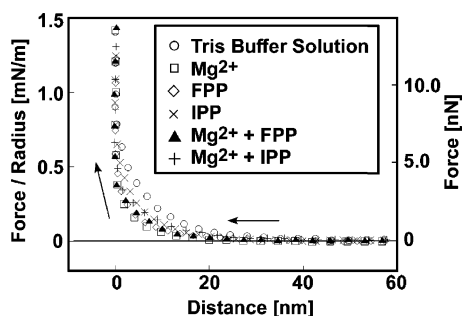


Figure 4. Force profiles of interactions between subunit I and subunit I surfaces upon approach under various condition at pH = 8.3: ○, 0.1 mM Tris buffer solution containing 1.0 mM NaCl; □, 0.1 mM Tris buffer solution containing 1.0 mM NaCl and 0.1 mM Mg²⁺; ◇, 0.1 mM Tris buffer solution containing 1.0 mM NaCl and 15 μM FPP; ×, 0.1 mM Tris buffer solution containing 1.0 mM NaCl and 15 μM IPP; ▲, 0.1 mM Tris buffer solution containing 1.0 mM NaCl, 0.1 mM Mg²⁺, and 15 μM FPP; +, 0.1 mM Tris buffer solution containing 1.0 mM NaCl, 0.1 mM Mg²⁺, and 15 μM IPP.

of subunit II. The QCM data in Figure 3 for the presence of Mg²⁺ showed that the binding of FPP with subunit II, most probably mediated by Mg²⁺, was more efficient than the FPP binding with subunit I by the hydrophobic interaction. It is interesting that the binding efficiency of FPP decreases in the presence of Mg²⁺, though we do not know the reason. The association constant of FPP with a subunit was estimated to be 5.7×10^4 and $1.1 \times 10^5 \text{ mol}^{-1}$ for subunit I and subunit II in the presence of 1.0 mM Mg²⁺, respectively, based on the Langmuir adsorption isotherm analysis.

Interactions between Identical Subunits: I and I; II and II. First, we measured the interaction between identical subunits as a control experiment. Figure 4 shows the interaction forces between subunits I and I upon approach at pH = 8.3. The separation distance of zero ($D = 0 \text{ nm}$) was set at the separation where the protein layers were no longer further compressed. Only a repulsive force was observed in 0.1 mM Tris buffer solution containing 1.0 mM NaCl at pH = 8.3. The isoelectric point of subunit I is known to be 5.1.¹⁶ Therefore, subunit I must be negatively charged in the solution at pH = 8.3, giving rise to the repulsive double layer force. Indeed, the observed repulsive force was described by an exponential function as expected for the double layer force, and its decay length of $9.2 \pm 0.3 \text{ nm}$ was in good agreement with the Debye length of 9.2 nm calculated for the corresponding salt concentration of 1.1 mM.³³ Upon separation, only repulsive forces were observed similar to the approach. In the 0.1 mM Tris buffer solutions containing (1) 1.0 mM NaCl at pH = 8.3, (2) 1.0 mM NaCl and 0.1 mM Mg²⁺ at pH = 8.3, (3) 1.0 mM NaCl, 0.1 mM Mg²⁺ and 15 μM FPP at pH = 8.3, (4) 1.0 mM NaCl, 0.1 mM Mg²⁺ and 15 μM IPP at pH = 8.3, (5) 1.0 mM NaCl and 15 μM FPP at pH = 8.3, and (6) 1.0 mM NaCl and 15 μM IPP at pH = 8.3, only repulsive forces were similarly observed both upon approach and separation.

These results show that (1) the proteins were charged at pH = 8.3 upon approach and (2) the nonspecific attraction was small and dominated by the double layer force. The same result was also obtained for subunit II with the isoelectric point of 5.2.

We calculated the surface charge densities for the interaction of subunit I and subunit II in the Tris buffer solution at pH = 8 using the theoretical formula of the electric double layer force.³⁴ The surface charge densities calculated from the force between subunits I and I and subunits II and II were $1.1 \times$

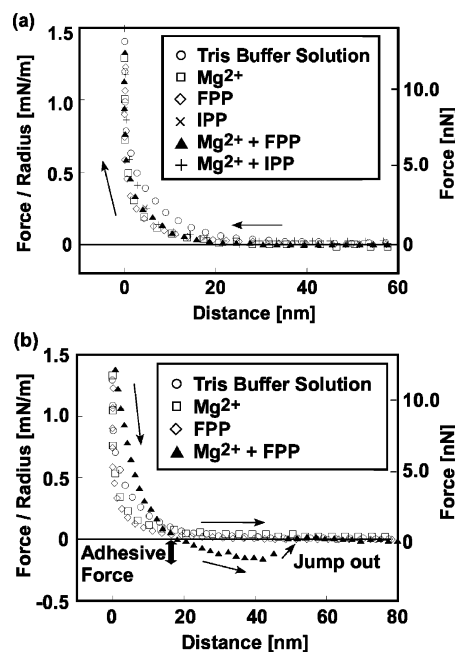


Figure 5. Force profiles of interactions between subunit I and subunit II surfaces a) upon approach b) upon separation under various condition at pH = 8.3. ○, 0.1 mM Tris buffer solution containing 1.0 mM NaCl; □, 0.1 mM Tris buffer solution containing 1.0 mM NaCl and 0.1 mM Mg²⁺; ◇, 0.1 mM Tris buffer solution containing 1.0 mM NaCl and 15 μM FPP; ×, 0.1 mM Tris buffer solution containing 1.0 mM NaCl and 15 μM IPP; ▲, 0.1 mM Tris buffer solution containing 1.0 mM NaCl, 0.1 mM Mg²⁺ and 15 μM FPP; +, 0.1 mM Tris buffer solution containing 1.0 mM NaCl, 0.1 mM Mg²⁺ and 15 μM IPP.

10^{-2} and $1.2 \times 10^{-2} \text{ charge/nm}^2$, respectively. These densities correspond to -0.77 and $-0.71 \text{ charge/protein}$ for subunit I and subunit II. On the other hand, the calculated charge based on the amino acid sequence of subunit I using GENETYX is about $-3.0 \text{ charge/protein}$. This difference seems reasonable: The surface charge calculated from the double-layer force profile could be smaller than the value estimated from the amino acid sequence, because neutralization of the surface charges by concentrations could generally occur.

Interactions between Subunit I and Subunit II upon Approach. Next, we directly measured the interaction between subunit I and subunit II, which were respectively immobilized on the substrate surfaces using the colloidal probe AFM. Figure 5a shows the interaction forces between subunits I and II upon approach at pH = 8.3. Only a repulsive force was observed in the 0.1 mM Tris buffer solution containing 1.0 mM NaCl at pH = 8.3, which is natural because both subunits were negatively charged at pH = 8.3, giving rise to the repulsive double-layer force. Indeed, the observed repulsive force was described by an exponential function as expected for the double-layer force, and its decay length of $9.2 \pm 0.4 \text{ nm}$ was in good agreement with the Debye length of 9.2 nm calculated for the corresponding salt concentration of 1.1 mM.³³

In the 0.1 mM Tris buffer solutions containing (1) 1.0 mM NaCl at pH = 8.3, (2) 1.0 mM NaCl and 0.1 mM Mg²⁺ at pH = 8.3, (3) 1.0 mM NaCl, 0.1 mM Mg²⁺ and 15 μM FPP at pH = 8.3, (4) 1.0 mM NaCl, 0.1 mM Mg²⁺ and 15 μM IPP at pH = 8.3, (5) 1.0 mM NaCl and 15 μM FPP at pH = 8.3, and (6) 1.0 mM NaCl and 15 μM IPP at pH = 8.3, there was almost no change in the surface force profiles.

(34) Chan, D. Y. C.; Pashley, R. M.; White, L. R. *J. Colloid Interface Sci.* **1980**, *77*, 283.

We calculated the surface charge densities for the interaction of subunit I and subunit II in the Tris buffer solution at pH = 8 using the theoretical formula of the electric double-layer force.³⁴ The surface charge densities calculated from the force between subunits I and II were 1.2×10^{-2} charge/nm², assuming that both surfaces have the same charges. This value is consistent with the surface charge densities calculated from the force between subunits I and I and subunits II and II, 1.1×10^{-2} and 1.2×10^{-2} charge/nm², respectively.

Interactions between Subunit I and Subunit II upon Separation. Figure 5b displays the surface forces between subunits I and II upon separation at pH = 8.3. In the 0.1 mM Tris buffer solution containing (1) 1.0 mM NaCl at pH = 8.3, (2) 1.0 mM NaCl and 0.1 mM Mg²⁺ at pH = 8.3, (3) 1.0 mM NaCl, 0.1 mM Mg²⁺ and 15 μM IPP at pH = 8.3, (4) 1.0 mM NaCl and 15 μM FPP at pH = 8.3, and (5) 1.0 mM NaCl and 15 μM IPP at pH = 8.3, the interaction was always repulsive. However, in the 0.1 mM Tris buffer solution containing 1.0 mM NaCl, 0.1 mM Mg²⁺, and 15 μM FPP at pH = 8.3, adhesive forces were observed upon separation though the repulsive force was observed upon approach. The intensity of the apparent adhesive force as shown in Figure 5b was 0.20 mN/m. This value was constant for the piezo driving velocities of 70–720 nm/s. We used the ‘‘apparent adhesive force’’ because we did not count the elastic force that appeared in the force profile before the jump-out. If the elastic force of a protein is considered, the actual adhesive force could be greater. However, it is not very easy to include this deformation; therefore, we used the apparent value.

The interactions between identical proteins (subunits I and I or subunits II and II) were always repulsive in all the solutions studied. Therefore, the observed adhesive force could be attributed to the specific interaction between subunits I and II which were associated by Mg²⁺ and FPP. Our observation agreed well with the report that a catalytically active complex is formed only in the presence of FPP and Mg²⁺ (Figure 1a).¹⁶ Thus, it is likely that we could form the intermediate complex by bringing the two subunits into contact by AFM and detect the adhesive force that possibly bridged the subunits by FPP and Mg²⁺.

Binding of Subunits I and II with DSIDA Monolayers Studied by QCM. The LB technique was used for preparing the sample surfaces, which consisted of two self-assembling LB layers adsorbing an additional protein layer. Therefore, it is necessary to determine which part of the layer assemblies was separated to give the observed adhesive force. We determined the association constants between each layer using the QCM. First, the adsorption amount of each subunit on the surface of the DSIDA-Cu²⁺ monolayer was measured. The

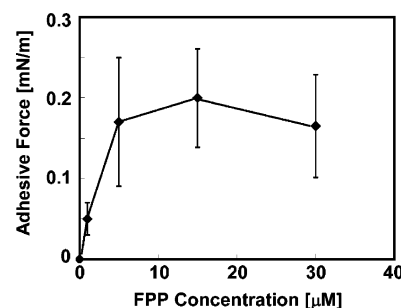


Figure 6. Adhesive force between subunits I and II versus the FPP concentration in the 0.1 mM Tris buffer solution containing 1.0 mM NaCl, 1.0 mM Mg²⁺, and 0–30 μM FPP at pH = 8.3.

association constant of a subunit and DSIDA-Cu²⁺ was estimated to be 0.7×10^7 and 1.4×10^7 mol⁻¹ for subunit I and subunit II, respectively (data not shown).³⁵ From a comparison of these association constants, the association between subunit I and FPP, 5.7×10^4 mol⁻¹, was the weakest of all the association in the multilayers. It has been known that the hydrophobic interaction between the first and second layers is in the range of 200–300 mN/m,^{36,37} much stronger than the adhesion discussed in this paper. Therefore, the observed adhesive force should correspond to the interaction force between subunit I and FPP, which is the weakest among these interactions. We estimated the number of adsorbed protein molecules per unit area using the QCM data and contacting area. The number of proteins in the contacting area is estimated to be 1400 for subunit I and 1700 for subunit II.³⁸

FPP Concentration Dependency on Specific Interaction.

To investigate whether the obtained adhesive force was the interaction between subunit I and subunit II, the FPP concentration dependency on the specific interactions between subunit I and subunit II was measured. The measurement was carried out in the 0.1 mM Tris buffer solution containing 1.0 mM NaCl, 1.0 mM Mg²⁺, and 0–30 μM FPP at pH = 8.3. Figure 6 plots the adhesive force between subunits I and II versus the FPP concentration. When the FPP concentration increased to 15 μM, the intensity of the average adhesive force became almost constant. This tendency is consistent with the QCM observation that FPP adsorption amounts bound to subunit II became constant at 15 μM. When the FPP concentration was further increased, the average adhesive force seemed to decrease to some extent, though the decrease was within the experimental error. If such decrease existed, it is consistent with the QCM observation that FPP started to bind to subunit I at FPP concentrations higher than 15 μM, which should suppress the complex formation shown in Figure 1b. These results provide another support for the fact that we could detect the adhesive force that bridged the subunits by FPP and Mg²⁺.

(35) The reliability of QCM measurement for studying the protein adsorption was examined by comparing the QCM data with the AFM images. We studied the AFM images and QCM data of a poly(histidine) tagged Sigma A proteins adsorbed to DSIDA monolayer.³⁹ The density of adsorbed Sigma A based on the AFM imaging was 1.5 proteins/(100 nm²). On the other hand, the estimated density of Sigma A using the QCM data was 1.8 ± 0.4 proteins/(100 nm²). These two values agree well to each other, indicating the reliability of QCM for estimating the amount of adsorbed proteins. The previous study using QCM demonstrated that the hydration mass is less than 10% of the molecular weight of the protein (lysozyme).⁴⁰ Our data of Sigma A also agree with this report if we assume the difference between QCM and AFM based values is due to the hydration. Therefore, we think that we can reasonably estimate the adsorbed amount of proteins based on the QCM data because in this study we used water soluble proteins similar to Sigma A and lysozyme. About FPP, the influence of hydration should be much less because FPP has a long hydrophobic tail.

(36) Claesson, P. M.; Christenson, H. K. *J. Phys. Chem.* **1988**, *92*, 1650.

(37) Kurihara, K.; Kunitake, T. *J. Am. Chem. Soc.* **1992**, *114*, 10927.

(38) To estimate the number of interacting molecules, we need to know the contact area, which is not possible to be directly determined in the case of AFM measurements. For SFA, we could determine the contacting area using the fringes of equal chromatic order (FECO). For example, the area providing adhesion force of 6.0×10^6 nN was 8.7×10^{-10} m² for hydrophobic mica surfaces.³⁷ The hydrophobic glass–plate surfaces used in our AFM measurement exhibited the adhesive force of 740 nN. Assuming that this difference is only due to the difference in the contacting area, we can estimate the contacting area to be 1.0×10^{-13} m² for our AFM measurement.

(39) Kurihara, K.; Suzuki, T.; Ishiguro, R. *Proc. OUMS* **2004**, 137.

(40) Smith, A. L.; Shirazi, H. M.; Mulligan, S. R. *Biochim. Biophys. Acta* **2002**, *1594*, 150.

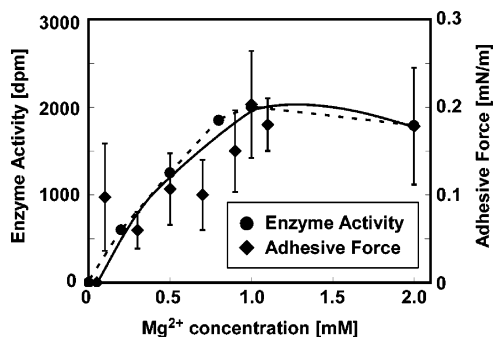


Figure 7. Average adhesive force and the enzyme activity between subunits I and II versus the Mg²⁺ concentration: ●, enzyme activity in the 25 mM Tris buffer solution containing 25 mM NH₄Cl, 10 mM 2-mercaptoethanol, 0–2.0 mM Mg²⁺, 15 μM FPP, and 0.3 μM [1-¹⁴C]IPP (1.95 TBq/mol) at pH = 8.5;²⁴ ◆, the average adhesive force in the 0.1 mM Tris buffer solution containing 1.0 mM NaCl, 0–2.0 mM mM Mg²⁺, and 15 μM FPP at pH = 8.3.

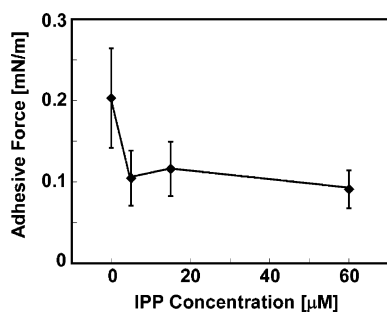


Figure 8. Average adhesive force between subunits I and II versus the IPP concentration in the 0.1 mM Tris buffer solution containing 1.0 mM NaCl, 1.0 mM Mg²⁺, 15 μM FPP, and 0–60 μM IPP at pH = 8.3.

Mg²⁺ Concentration Dependency on Specific Interaction.

The enzyme activity is changed by the Mg²⁺ concentration according to Zhang et al.²⁴ It is reasonable to assume that the enzyme activity should be directly related to the formation of an enzyme–substrate complex, that is, the adhesive force observed in the presence of FPP and Mg²⁺. To investigate their correlation, we measured the Mg²⁺ concentration dependence of the adhesive forces between subunits I and II in the 0.1 mM Tris buffer containing 1.0 mM NaCl, 0–2.0 mM Mg²⁺, and 15 μM FPP at pH = 8.3. These results are shown in Figure 7 together with the Mg²⁺ concentration dependence of the enzyme activity. The intensity of the apparent adhesive force increased with the Mg²⁺ concentration change. No adhesive force was observed at the Mg²⁺ concentration of 0 mM and 0.05 mM. The adhesive forces began to be detected at 0.1 mM Mg²⁺ and became a maximum at 1.0 mM Mg²⁺. Similarly, the enzyme activity also exhibited the maximum value at 1.0 mM Mg²⁺. Both values simultaneously changed, though the errors in the average adhesive force were large. This result also supported the fact that we could detect one of the reaction intermediates of HepPP synthase, the subunit complex by FPP and Mg²⁺.

Effect of IPP on Specific Interaction. To investigate how the interactions between subunits I and II change when FPP and the second substrate IPP were both present in the solution, the effect of IPP on the specific interactions was measured. Figure 8 shows the IPP concentration dependence of the average adhesive forces in the 0.1 mM Tris buffer solution containing 1.0 mM Mg²⁺, 15 μM FPP and 0–60 μM IPP at pH = 8.3. In the presence of FPP and IPP, the adhesive force decreased to about half of the value for the presence of only FPP. When the

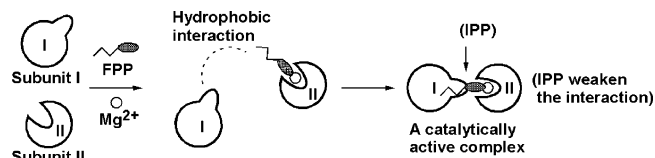


Figure 9. Proposed mechanism for the formation of the catalytically active complex of HepPP synthase.

IPP concentration was increased to 60 μM, the adhesive force was constant. Based on the hypothetical mechanism of HepPP synthase (Figure 1a), this enzyme–substrate complex catalyzes the consecutive condensation of FPP and four molecules of IPP to produce HepPP. Though a precise mechanism of how the HepPP synthase elongates the chain length has not yet been clarified, some kind of binding in the enzyme–substrate complex must be broken (Figure 1b). Therefore, the decreasing of the adhesive forces in the presence of both FPP and IPP should be ascribed to the destabilization of the complex. This result also provided evidence that we could detect the intermediate state of HepPP synthase using colloidal probe AFM.

Proposed Mechanism of Complexation. Taken together, it seems that a more likely scenario for the formation of the complex first involves binding of FPP–Mg²⁺ with subunit II and the subsequent association of subunit I. In the AFM results, we observed the adhesive forces between subunit I and subunit II only in the presence of both Mg²⁺ and FPP. The QCM data in Figure 3 for the presence of Mg²⁺ showed that the binding of FPP with subunit II, the most probably mediated by Mg²⁺, was more efficient than the FPP binding with subunit I by a hydrophobic interaction. The complex formation process from these results is schematically shown in Figure 9.

Conclusion

In this research, we studied the molecular mechanism of an enzyme reaction, which is a complicated biological reaction, using AFM and QCM. The binding site of the substrate was determined using QCM. By using the LB method, subunits I and II of HepPP synthase were immobilized on glass surfaces, and the interaction between them was directly measured using the colloidal probe AFM. It was possible, for the first time, to detect the interactions involved in the complex formation of the enzyme subunits, a cofactor and a substrate (FPP in our case). Furthermore, we demonstrated that the adhesive force and the catalytic activity simultaneously changed when the Mg²⁺ concentration was varied, and the IPP may destabilize the substrate–enzyme complex, thus decreasing the adhesive force. These results supported the fact that the observed adhesive forces were involved in the catalytic reaction, and a possible mechanism of the substrate–enzyme complexation was proposed. This study demonstrated a very useful methodology for examining the elemental processes of biological reactions, such as an enzyme reaction.

Acknowledgment. This work was partially supported by Grant-in-Aids for 21st century COE Research, Giant Molecules and Complex Systems, from the Ministry of Education, Culture, Sports, Science and Technology of Japan and supported by the CREST program of Japan Science and Technology Agent.

JA061822K